Archival Report

Biological Psychiatry: CNNI

Divergent Network Patterns of Amyloid-β Deposition in Logopenic and Amnestic Alzheimer's Disease Presentations

Cristian E. Leyton, Ben Cassidy, Victor L. Villemagne, Gareth Jones, John B. Kwok, Christopher C. Rowe, Kirrie J. Ballard, Olivier Piguet, and John R. Hodges

ABSTRACT

BACKGROUND: Despite divergent clinical features, language and amnestic presentations of Alzheimer's disease (AD) appear to show comparable regional amyloid-β (Aβ) burden. By using a statistical network approach, we aimed to identify complex network patterns of Aβ deposition and explore the effect of apolipoprotein E (*APOE*) ε4 allele on cortical Aβ burden across AD phenotypes.

METHODS: Sixteen amnestic AD participants and 18 cases with logopenic-variant of primary progressive aphasia (lv-PPA) with a high cortical Aβ burden were selected. A comprehensive clinical assessment, Aβ imaging, and *APOE* genotyping were performed in all cases. Statistical network analysis was undertaken based on the estimation of sparse partial correlations of Aβ burden between cortical regions. Global and regional network statistical parameters as well as the effect of *APOE* ε4 genotype on cortical Aβ were explored.

RESULTS: The two groups showed equivalent distribution of cortical amyloid burden and frequency of *APOE* ε4 genotype. Statistical network analysis, however, demonstrated divergent connectivity properties. The lv-PPA group demonstrated higher mean network degree and shorter characteristic path length than the amnestic AD group. Amnestic AD cases showed connectivity hubs confined to the mesial temporal and prefrontal lobes bilaterally, whereas lv-PPA cases showed hubs scattered across the whole cortical mantle. An interaction effect on total Aβ burden between *APOE* genotype and AD presentations was also detected.

CONCLUSIONS: The network analysis reveals interregional network differences not evident using a simple comparison of Aβ burden. This suggests that regional neurotoxic effects may explain the phenotypical differences in AD presentation and that these can be modulated by *APOE* genotype.

Keywords: Alzheimer's disease, Amyloid-β, Apolipoprotein E ε4, Complex network analysis, Logopenic variant of primary progressive aphasia, Pittsburgh Compound B positron emission tomography (PiB-PET)

http://dx.doi.org/10.1016/j.bpsc.2015.09.004

Alzheimer's disease (AD) is the most common neurodegenerative disorder, characterized pathologically by neuronal loss, deposition of amyloid-β (Aβ) plaques, and neurofibrillary tangles (1). Despite this shared neuropathological substrate, AD can manifest as different clinical phenotypes. The amnestic presentation, the most common clinical form, is typified by prominent episodic memory impairment and bilateral atrophy of temporal mesial structures. By contrast, the aphasic presentation, known as logopenic-variant of primary progressive aphasia (lv-PPA), displays prominent language deficits and atrophy in the left temporal parietal junction (2,3). In keeping with these clinical and neuroanatomical differences, pathologic evidence demonstrates that lv-PPA exhibits higher neurofibrillary density in the left temporoparietal cortex than amnestic AD cases (4,5).

Evidence for differential Aβ distribution obtained from Aβ imaging, however, reveals somewhat conflicting results. While most studies demonstrate no differences in the distribution of Aβ between AD presentations (6–9), a few reports have shown a distinctive topographical pattern of Aβ distribution in lv-PPA (10,11). These conflicting results confirm the heterogeneity of the disease and illustrate the complex interactions between local Aβ accumulation and neurotoxicity. Consequently, rather than the direct Aβ quantification, analysis of regional covariation of Aβ can potentially offer a better account for complex patterns of regional interaction not evident otherwise (12). In this way, statistical network analysis using graph theoretical methods (13) provides a suitable framework to investigate complex topological properties of Aβ distribution across AD presentations on the grounds that regions with a high degree of covariation may share common pathologic events. This presumption is in keeping with the idea that Aβ accumulation does not occur in a diffuse or at constant rate, but rather occurs in the cortical mantle at different rates (14,15). Accordingly, regions showing similar Aβ variability, even if they are distant, may reflect common stages of the pathologic

cascade, thereby yielding a topologic pattern distinctive for each clinical phenotype.

Our primary aim was to analyze network properties of brain Aβ distribution in amnestic AD and lv-PPA cases with high cortical Aβ burden. We hypothesized that despite an equivalent distribution of Aβ, a statistical network analysis would reveal divergent spatial patterns in Aβ burden covariation. Given evidence that suggests the apolipoprotein E ε4 (*APOE* ε4) allele can modulate the neurotoxic effects of Aβ over neuronal function in AD (16), our secondary aim was to explore the interaction between AD presentations, *APOE* status, and Aβ burden.

METHODS AND MATERIALS

Participants

Consecutive participants with the clinical diagnosis of lv-PPA ($n = 18$) or amnestic AD ($n = 16$) were recruited from the frontotemporal dementia clinical research group in Sydney ($n = 26$) or from the Austin Hospital in Melbourne ($n = 8$), Australia. All cases fulfilled the current diagnostic criteria for lv-PPA (3) or amnestic AD (2) and demonstrated high ^{11}C-Pittsburgh Compound B (PiB) retention in at least one cortical region. This criterion was adopted in order to ensure nosologic consistency in both AD presentations, given that a proportion of cases with lv-PPA present with non-Alzheimer's pathology (17). High Aβ burden was regarded as a standardized uptake value ratio normalized to cerebellar cortex equal to or higher than 1.5 (18). The study received approval from the relevant human ethics committees.

Neuropsychological Evaluation

All participants were administered the Addenbrooke's Cognitive Examination Revised (19) to estimate their current global cognitive ability. This screening cognitive measure comprises items that evaluate attention and orientation, memory, verbal fluency, language, and visuospatial abilities. All participants also underwent the Sydney Language Battery (20), consisting of visual confrontation naming, multisyllabic word repetition, single-word comprehension, and semantic association tasks.

Determination of Apolipoprotein E ε4 Genotype

Technical details of this procedure are indicated in Supplementary Material in Supplement 1.

Positron Emission Tomography Imaging Acquisition

PiB positron emission tomography (PET) scans were acquired at the Austin Hospital on an Allegro PET camera (Philips, Amsterdam, The Netherlands) with a resolution of 5.0 × 5.0 × 6.5 mm^3 (x, y, z). A transmission scan was performed for attenuation correction. Each participant received ~370 MBq PiB intravenously over 1 minute. A 30-minute acquisition (6 × 5-minute frames) in three-dimensional mode starting 40 minutes after injection of PiB was performed. PET images were reconstructed using a three-dimensional row-action maximization-likelihood algorithm using a voxel size of 2.0 mm^3. Summed 40- to 70-minute images were used in each study.

Neuroimaging Data Processing

All imaging data sets were analyzed using SPM8 (Wellcome Trust Centre for Neuroimaging, London, UK; http://www.fil.ion.ucl.ac.uk/spm/) and PMOD 3.2 (PMOD Technologies Ltd, Zurich, Switzerland; http://www.pmod.com/technologies/products/products.html). PiB PETs were spatially normalized using the 12-parameter affine transformation defined by the SPM8 Normalize procedure to the subject's T1-weighted magnetic resonance image. The resulting gray-matter images were smoothed with an 8-mm kernel and these data were used to conduct contrasts between groups.

Twenty-two cortical regions (11 in each hemisphere) were defined as regions of interest (ROI) using an in-house atlas (18). Cortical PiB standardized uptake values were normalized using the cerebellar cortex as reference region, and the resulting regional standardized uptake value ratios were used for network construction.

Network Analysis of Brain Aβ Distribution

The network analyses conducted rely on the construction of binary-undirected adjacency matrices, one for each sample. Each adjacency matrix represents the pattern of amyloid intervariation across brain regions of the sample, whereby ROIs constitute nodes and nonzero entries are considered connections or links of the network (21). The binary values of the adjacency matrix were defined as the nonzero values resulting from sparse partial correlation estimation, an established method that enables the estimation of dependency between each of the ROI pairs conditional on the rest of ROIs in relatively small samples with larger number of variables (22). Estimating network links via partial correlations allows the Aβ network to be represented as a conditional independence graph. Conditional independence is a fundamental requirement for graphical modeling since network links then indicate the presence of direct interactions, rather than indirect interactions if a network were constructed using marginal Pearson correlations. The conditional independence graph can then be interpreted in a proper statistical framework (23).

Network Metrics

The binary adjacency matrices allowed the estimation of network topology metrics, which include the calculation of global network parameters at global and node level in each patient group. Global parameters include mean network degree and characteristic path length (21,24,25). The mean network degree is the average of the degree over all nodes, in which the degree of an individual node represents the number of links connected to that node. Individual values of the degree reflect the importance of nodes in the network. The characteristic path length of the graphs is the smallest number of connections required to connect one node to another, averaged over all pairs of nodes. We also explored assortative mixing coefficients, which represent the level of connection among nodes with similar degrees (26). In other words, a network with a positive assortative mixing coefficient means that nodes with similar degrees tend to connect to each other. By contrast, networks with a negative mixing coefficient or a dissortative mixing pattern have nodes with contrasting degrees that tend to connect to each other.

Network parameters at the local level were calculated for each node to identify its relevance in the network. In addition

Table 1. Demographic Characteristics of lv-PPA and AD Groups

	lv-PPA (n =18)	AD (n = 16)	Statistics	p
Female (%)	50%	38%	χ^2 = .5	ns
APOE ε4 (%)	39%	50%	χ^2 = .4	ns
Education, Years	13.3 ± 3.1	13.2 ± 3.4	t = −.1	ns
Age at Onset, Years	61.3 ± 6.9	60.9 ± 4.8	t = .6	ns
Age at Diagnosis, Years	63.6 ± 7.1	64.8 ± 5.3	t = −.2	ns
Age at Testing, Years	63.9 ± 6.9	65.4 ± 5.7	t = .7	ns

AD, Alzheimer's disease; lv-PPA, logopenic-variant of primary progressive aphasia; ns, nonsignificant.

to degree, we studied clustering coefficient, which is the number of connections between neighbors of a given node divided by all their possible connections (27). The other local parameter calculated for each node was betweenness centrality (28), which is the proportion of all shortest paths in the network that pass through a given node. Those nodes within the 70th percentile in at least two of the centrality measures were regarded as hubs.

RESULTS

Demographic Features, Onset, and *APOE* Genotype

Both lv-PPA and AD groups demonstrated comparable demographic features, age at onset, age at diagnosis, and *APOE* ε4 allele frequency, either homozygote or heterozygote (Table 1).

Cognitive Performance

Both groups scored below the cutoff of 82 on the Addenbrooke's Cognitive Examination Revised, denoting presence of cognitive impairment (19). The lv-PPA group scored lower than AD due to their poorer performance on language-based items. Similarly, lv-PPA also scored lower than AD in the Sydney Language Battery naming and word repetition. By contrast, both groups experienced similar functional impairment (Table 2).

Aβ Burden

As shown in Figure 1, no significant differences in regional PiB retention were present between AD and lv-PPA (two-tailed unpaired t tests for each region). An analysis of variance of the

Table 2. Cognitive and Single-Word Performance in lv-PPA and AD Patients

	lv-PPA	AD	Statistics	p
ACE-R Total / 100	65.2 ± 11.4	73.8 ± 12.7	t = 2.1	.047
Attention and orientation / 18	15.0 ± 2.8	15.1 ± 2.6	t = .1	ns
Memory / 26	14.6 ± 5.9	15.9 ± 5.0	t = .7	ns
Fluency / 14	5.2 ± 2.5	7.8 ± 3.3	t = 2.6	.014
Language / 26	16.8 ± 4.8	21.8 ± 3.9	t = 3.2	.003
Visuospatial / 16	13.6 ± 2.1	13.2 ± 3.3	t = −.4	ns
Sydbat				
Naming / 30	14.5 ± 7.0	21.1 ± 5.4	z = −2.7	.006[a]
Word comprehension / 30	26.8 ± 1.9	26.2 ± 2.8	z = −.1	.721[a]
Semantic association / 30	25.6 ± 1.8	25.4 ± 3.1	z = −.4	.932[a]
Word repetition / 30	25.9 ± 5.5	29.7 ± .7	z = −3.9	<.001[a]
FRS Rasch Score	1.4 ± 1.8	.8 ± .9	t = −1.0	ns

ACE-R, Addenbrooke's Cognitive Examination Revised; AD, Alzheimer's disease; FRS, Frontotemporal Dementia Ratio Scale; lv-PPA, logopenic-variant of primary progressive aphasia; ns, nonsignificant; Sydbat, Sydney Language Battery.
[a]Mann-Whitney test.

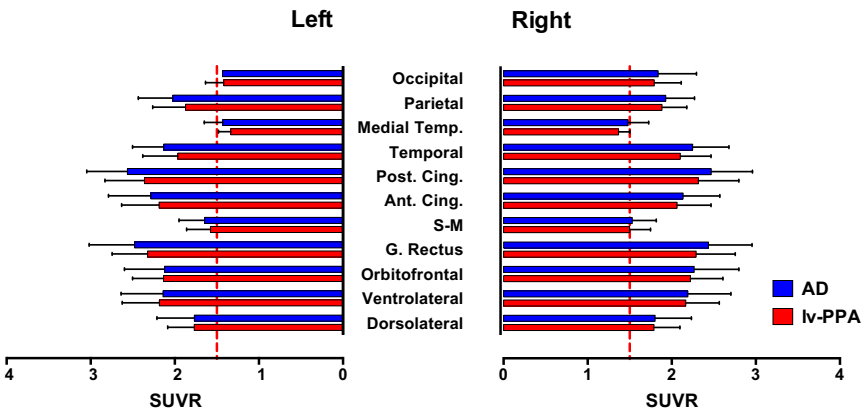

Figure 1. Pittsburgh Compound B standardized uptake value ratio (SUVR) means (x axis) are presented for each cortical region and diagnostic group (y axis). The red dashed lines indicate the threshold separating high from low Pittsburgh Compound B retention. Pairwise comparisons between lv-PPA and amnestic AD across all cortical regions rendered nonsignificant results. AD, Alzheimer's disease; Ant. Cing., anterior cingulate; Dorsolateral, dorsolateral prefrontal lobe; G. Rectus, gyrus rectus; lv-PPA, logopenic-variant of primary progressive aphasia; Medial Temp., medial temporal lobe; Orbitofrontal, orbital frontal lobe; Post. Cing., posterior cingulate; S-M, sensorimotor cortex; Ventrolateral, ventrolateral prefrontal lobe.

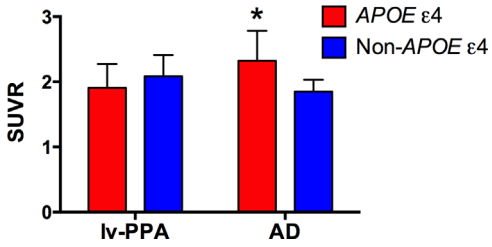

Figure 2. Means for neocortical standardized uptake value ratio (SUVR) of Pittsburgh Compound B display for each diagnostic subgroup divided according to the presence of the apolipoprotein E ε4 (*APOE* ε4) allele. The asterisk (*) identifies the subgroup that demonstrated the significantly higher amyloid-β burden. AD, Alzheimer's disease; lv-PPA, logopenic-variant of primary progressive aphasia.

total cortical PiB retention (i.e., the average of the bilateral frontal, parietal, lateral temporal, lateral occipital, and anterior and posterior cingulate regions) was conducted to investigate the differential effect of diagnostic group, *APOE* ε4 status, and interactive effects on total cortical Aβ retention. This analysis showed no main effects of diagnosis ($F_{1,30} = .56$, $p = .5$) or *APOE* ε4 status ($F_{1,30} = 1.5$, $p = .2$) on neocortical Aβ burden but a significant diagnosis by *APOE* ε4 status interaction ($F_{1,30} = 7.3$, $p = .01$). The post hoc pair-wise contrasts with Bonferroni corrections demonstrated that AD cases with *APOE* ε4 allele had higher neocortical Aβ burden (2.32) than AD cases without *APOE* ε4 allele (1.85, $p = .01$) and than lv-PPA cases with *APOE* ε4 allele (1.91, $p = .03$) (Figure 2).

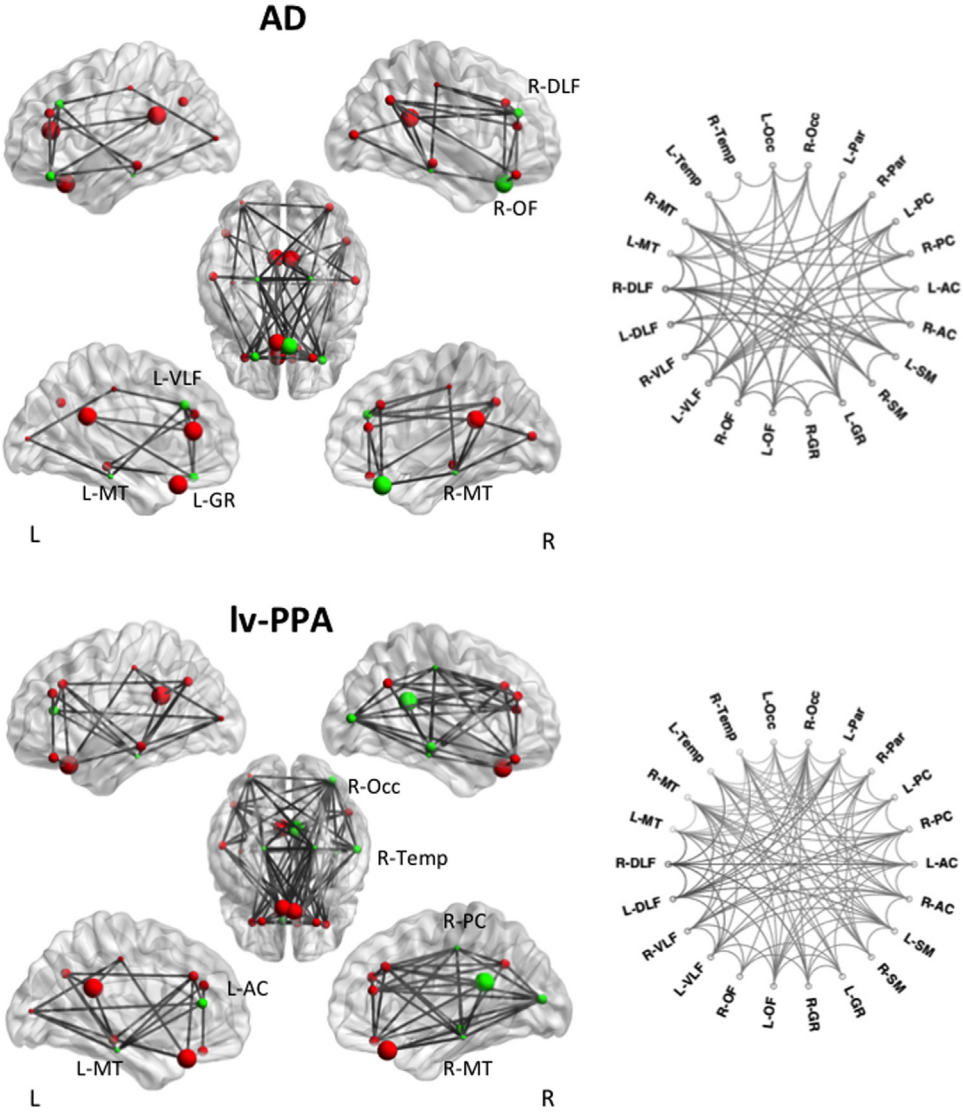

Figure 3. Aβ networks representation for amnestic Alzheimer's disease (AD) and logopenic-variant of primary progressive aphasia (lv-PPA). On the left side, nodes and links are mapping onto a brain model. The size of nodes indicates the relative Aβ burden. Large nodes indicate nodes over the 70th percentile, corresponding approximately to standardized uptake value ratio Pittsburgh Compound B (SUVR-PiB) > 2.28, whereas small nodes indicate low Aβ burden, placed under the 30th percentile, corresponding to SUVR-PiB < 1.7. Green nodes represent hubs (see Table 4 for more details). On the right, Aβ networks are presented in circular graphs. AC, anterior cingulate; DLF, dorsolateral frontal; GR, gyrus rectus; L, left; MT, mesial temporal; Occ, occipital; OF, orbitofrontal; Par, parietal; PC, posterior cingulate; R, right; SM, sensory motor cortex; Temp, temporal; VLF, ventrolateral frontal.

Table 3. Global Network Parameters in lv-PPA and AD Groups

	lv-PPA	AD
Nodes	22	22
Edges	102	65
Mean Network Degree[a]	9.3	5.9
Mean Clustering Coefficient[a]	.4	.3
Characteristic Path Length[a]	1.5	1.8
Mixing Assortativity	−.01	−.17

AD, Alzheimer's disease; lv-PPA, logopenic-variant of primary progressive aphasia.

[a]$p < .001$, Mann-Whitney test.

Statistical Network Analysis

Aβ network representations are displayed in Figure 3. Global network parameters demonstrated higher mean network degree and shorter characteristic path length in the lv-PPA group than in amnestic AD (Table 3). In accordance with these global parameters, the cumulative distribution displayed in Figure 4 indicated that the proportion of nodes with a high degree was higher in lv-PPA than in the amnestic AD group. In addition, the lv-PPA group evidenced absence of assortativity; that is to say, degree did not influence connections between nodes. By contrast, the AD group showed a trend of dissortative mixing pattern whereby high-degree nodes preferentially connected with low-degree nodes.

Spearman rank-order correlations were undertaken to investigate whether an association was present between regional Aβ burden and centrality parameters. With the exception of node degree in lv-PPA, which showed a significant correlation with Aβ burden ($\rho = -.44$, $p = .04$), none of them reached significant association in either group (Table S1 in Supplement 1).

Although both groups shared hubs in the mesial temporal cortices, they demonstrated a divergent anatomical distribution of hubs throughout the remaining cortical mantle (Table 4). In amnestic AD, hubs were located in frontal lobes bilaterally, while in lv-PPA, hubs were distributed in predominantly left lateralized posterior cortical regions.

DISCUSSION

Using network statistical analyses, we compared the distribution of brain Aβ in AD cases with either an amnestic presentation or a logopenic syndrome. While the direct comparison of regional Aβ burden revealed no group differences, confirming previous reports (6,7,29), the network statistical analyses revealed differences in parameters at global and regional levels.

In amnestic AD presentation, most nodes had low degrees, and the few nodes that had high degrees tended to connect to nodes with low degrees (negative assortative mixing correlation). By contrast, the network degree distribution in lv-PPA was close to a normal distribution in which the proportion of high-degree nodes was equivalent to that of low-degree nodes, while the largest proportion had intermediate values of degree. The absence of assortativity mixing correlation in lv-PPA indicates that connections between nodes tend to be random. These differences in global network parameters suggest that the pattern of regional amyloid covariance is more generalized and diffuse in lv-PPA than in amnestic AD, whereby a large number of regions share common pathophysiological processes in the former and a few regional foci seem to play a major role in the latter. Accordingly, the analysis of hubs demonstrated that core regions in the amnestic AD patients were located bilaterally in the frontal lobes, including both orbital frontal cortices. This regional pattern of hubs regions is thought to play a role in the putative spreading mechanisms in early stages of AD pathology, as suggested in another study using a similar approach (12).

Despite sharing common hubs with amnestic AD cases, lv-PPA cases had a different distribution of hubs characterized by involvement of posterior cortical regions, including occipital and temporal cortices. This finding not only corroborates the common pathological involvement of mesial temporal cortices in both AD presentations (4), but also highlights the distinctive pattern of lv-PPA in which Aβ burden in posterior cortical regions seems to confer a distinctive phenotype in lv-PPA (11). In keeping with these findings, a prior study using structural covariance analysis (30) found two dissociable patterns of brain atrophy in healthy older individuals with positive PiB retention, suggesting a selective network involvement. Of importance, most nodal parameters were not correlated with Aβ burden, indicating that the emergence of hubs is independent of Aβ burden and that distant regions can share common pathophysiological dynamics irrespective of their Aβ burden (31). Nevertheless, lv-PPA group showed a negative correlation between node degree and Aβ burden, suggesting that earlier stages of pathological processes are more likely to be occurring in high-degree nodes than in low-degree nodes

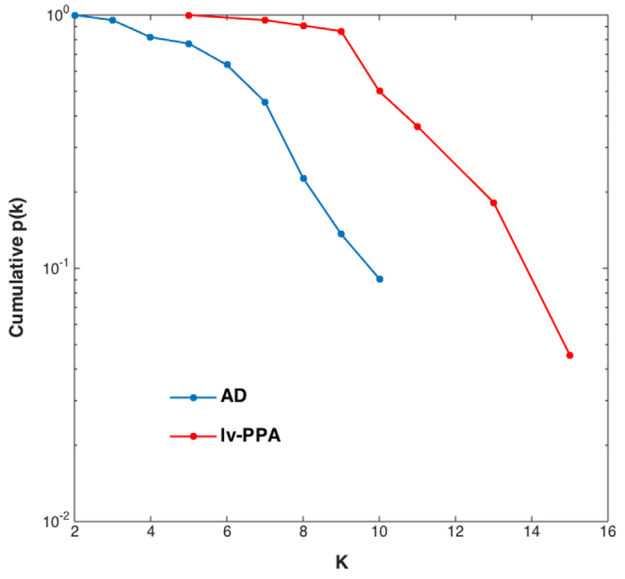

Figure 4. Cumulative probability distribution of node degrees for Alzheimer's disease (AD) and logopenic-variant of primary progressive aphasia (lv-PPA) presented in a semi-logarithmic scale. The horizontal axis represents the degree value (K) and the vertical axis is the cumulative probability of degrees p(k), that is to say, the probability of nodes that have degree greater than or equal to k.

Table 4. Hub Statistical Parameters in lv-PPA and AD Groups

lv-PPA					AD				
Region	SUVR	Degree	Betweenness	Clustering Coefficient	Region	SUVR	Degree	Betweenness	Clustering Coefficient
Left Mesial Temporal	1.33	11	13.2	.49	Left Ventrolateral Prefrontal	2.14	10	62.7	.18
Right Mesial Temporal	1.37	13	24.6	.40	Right Orbitofrontal	2.27	8	43.7	.25
Right Posterior Cingulate	2.32	10	16.1	.38	Left Rectus Gyrus	2.48	9	36.3	.28
Left Anterior Cingulate	2.19	10	9.6	.53	Right Dorsolateral	1.80	9	32.1	.19
Left Sensory Motor	1.58	10	10.7	.51	Left Mesial Temporal	1.43	7	29.58	.24
Right Temporal	2.10	10	15.6	.44	Right Mesial Temporal	1.80	9	32.1	.19
Right Occipital	1.79	15	36.7	.42					

AD, Alzheimer's disease; lv-PPA, logopenic-variant of primary progressive aphasia; SUVR, standardized uptake value ratio.

in lv-PPA. This relationship was not found in amnestic AD cases, suggesting again topological differences in both groups on the neurotoxic effect of Aβ burden. These results raise fundamental questions concerning the relation between Aβ deposition, neuronal dysfunction, and clinical symptoms, suggesting that Aβ deposition is a necessary but not a sufficient condition to cause neuronal damage. Multiple studies have shown that this relationship between Aβ and brain atrophy is not direct or robust, suggesting that other, as yet unknown, variables are involved in the development of neurodegeneration (14, 32–34). Network analysis can provide a complementary perspective to understand this relationship. In accordance with this perspective, some evidence suggests that Aβ deposits are biochemically and morphologically heterogeneous (35,36), resulting in phenotypical differences in AD despite equivalent Aβ distribution, such as the language presentation (37). Although current imaging techniques of Aβ radiotracers correspond closely with the stereotypical regional progression of Aβ accumulation in postmortem samples (38), these techniques are not yet able to detect molecular subtypes of amyloid.

Another finding of interest was the interaction effect between diagnosis and *APOE* status, suggesting a complex interplay between *APOE* genotype and clinical phenotype. Although carriers of the *APOE* ε4 allele are associated with higher risk for AD, this association is less clear in lv-PPA. Some reports have shown no association of this genotype with lv-PPA (39,40), although this finding is not universal (41). Several variables, including inherent clinical heterogeneity of lv-PPA (42), may account for this discrepancy. Our findings, however, suggest that *APOE* ε4 has an effect on the Aβ burden in cases with amnestic AD presentation but not in those with language presentation. Although the association of *APOE* ε4 with higher Aβ burden has been shown in AD (43), the mechanisms operating in this differential effect in lv-PPA are unknown and warrant further research.

The small sample sizes may have limited the network statistical analysis. This issue, however, was minimized by the inference of sparse partial correlations (22), a novel approach that allows the identification of hubs in a high-dimension, low sample size setting. In addition, the selection of key cortical regions as nodes likely minimized the effect of high dimensionality of the setting. Inferential statistical methods in complex network analysis remain in a developmental stage and our findings will benefit from replication in a larger data set.

Despite these potential limitations, network analysis reveals intricate interregional interactions not evident with the direct comparison of Aβ burden. In addition, our findings suggest the existence of particular regional patterns that might account for the clinical heterogeneity in AD, and certainly, they suggest that *APOE* status plays a role in the modulation of Aβ neurotoxicity.

ACKNOWLEDGMENTS AND DISCLOSURES

This work was supported by a National Health and Medical Research Council (NHMRC) Project Grant (Grant No. 630489); Forefront NHMRC Program Grant project (Grant No. 1037746); the Australian Research Council (ARC) Centre of Excellence in Cognition and its Disorders (Grant No. CE110001021); a Sydney University Postdoctoral Fellowship (Grant No. S0716/U2644 to CEL); an ARC Future Fellowship (Grant No. FT120100355 to KJB); an ARC Federation Fellowship (Grant No. FF0776229 to JRH); and an NHMRC Career Development Fellowship (Grant No. APP1022684 to OP).

We are grateful to the participants and their families for supporting our research. We thank the participants in the FRONTIER and Lauren Bartley for coordinating this research program.

A/Prof. Victor Villemagne reports a consultant fee for Novartis, speaker's honoraria from Piramal and GE Healthcare, and grant support from NHMRC Fellowship.

A/Prof. John B. Kwok was funded by NHMRC Project Grant APP1005769 but otherwise reports no biomedical financial interests or potential conflicts of interest.

Professor Christopher Rowe is a named inventor on a patent for automated analysis of amyloid positron emission tomography scans and has received speaker honoraria from Piramal Imaging and GE Healthcare.

A/Prof. Olivier Piguet reports funding support from The Australian Research Council and the National Health Medical Research Council of Australia. Dr. Piguet also serves on the Editorial Boards of Frontiers in Dementia Research, Frontiers in Emotion Science, and Behavioural Neurology.

Professor John Hodges reports funding support from National Health and Medical Research Council of Australia Program Grant, Australian Research Council Centre of Excellence in Cognition and its Disorders Memory Node; receives personal compensation in the form of publishing royalties for Cognitive Assessment for Clinicians (Oxford University Press, 2007) and Frontotemporal Dementia Syndromes (Cambridge University Press, 2007); and serves on the Editorial Boards of Nature Reviews Neurology, Aphasiology, Cognitive Neuropsychiatry, and Cognitive Neuropsychology.

All other authors report no biomedical financial interests or potential conflicts of interest.

ARTICLE INFORMATION

From the Faculty of Health Sciences (CEL, KJB), The University of Sydney, Lidcombe; Neuroscience Research Australia (CEL, JBK, OP, JRH), Randwick; and Australian Research Council Centre of Excellence in Cognition and its Disorders (CEL), Sydney, New South Wales, Australia; Department of Biostatistics (BC), Mailman School of Public Health, Columbia University, New York, New York; Department of Nuclear Medicine and Centre for PET (VLV, GJ, CCR), Austin Health, Heidelberg; The Florey Institute of Neuroscience and Mental Health (VLV), The University of Melbourne, Melbourne, Victoria; and School of Medical Sciences (OP, JRH), The University of New South Wales, Sydney, New South Wales, Australia.

Address correspondence to Cristian E. Leyton, Ph.D., The University of Sydney, Faculty of Health Sciences, 75 East St Libcombe, Sydney, NSW 2031, Australia; E-mail: cristian.leyton@sydney.edu.au.

Received Sep 8, 2015; accepted Sep 21, 2015.

Supplementary material cited in this article is available online at http://dx.doi.org/10.1016/j.bpsc.2015.09.004.

REFERENCES

1. Braak H, Braak E (1991): Neuropathological stageing of Alzheimer-related changes. Acta Neuropathol 82:239–259.
2. McKhann GM, Knopman DS, Chertkow H, Hyman BT, Jack CR Jr, Kawas CH, *et al*. (2011): The diagnosis of dementia due to Alzheimer's disease: Recommendations from the National Institute on Aging-Alzheimer's Association workgroups on diagnostic guidelines for Alzheimer's disease. Alzheimers Dement 7:263–269.
3. Gorno-Tempini ML, Hillis AE, Weintraub S, Kertesz A, Mendez M, Cappa SF, *et al*. (2011): Classification of primary progressive aphasia and its variants. Neurology 76:1006–1014.
4. Gefen T, Gasho K, Rademaker A, Lalehzari M, Weintraub S, Rogalski E, *et al*. (2012): Clinically concordant variations of Alzheimer pathology in aphasic versus amnestic dementia. Brain 135:1554–1565.
5. Josephs KA, Dickson DW, Murray ME, Senjem ML, Parisi JE, Petersen RC, *et al*. (2013): Quantitative neurofibrillary tangle density and brain volumetric MRI analyses in Alzheimer's disease presenting as logopenic progressive aphasia. Brain Lang 127:127–134.
6. Mendez MF, Sabodash V (2015): Clinical amyloid imaging in logopenic progressive aphasia. Alzheimer Dis Assoc Disord 29:94–96.
7. Lehmann M, Ghosh PM, Madison C, Laforce R Jr, Corbetta-Rastelli C, Weiner MW, *et al*. (2013): Diverging patterns of amyloid deposition and hypometabolism in clinical variants of probable Alzheimer's disease. Brain 136:844–858.
8. Leyton CE, Villemagne VL, Savage S, Pike KE, Ballard KJ, Piguet O, *et al*. (2011): Subtypes of progressive aphasia: Application of the international consensus criteria and validation using beta-amyloid imaging. Brain 134:3030–3043.
9. Rabinovici GD, Jagust WJ, Furst AJ, Ogar JM, Racine CA, Mormino EC, *et al*. (2008): Abeta amyloid and glucose metabolism in three variants of primary progressive aphasia. Ann Neurol 64:388–401.
10. Ng SY, Villemagne VL, Masters CL, Rowe CC (2007): Evaluating atypical dementia syndromes using positron emission tomography with carbon 11 labeled Pittsburgh Compound B. Arch Neurol 64: 1140–1144.
11. Whitwell JL, Lowe VJ, Duffy JR, Strand EA, Machulda MM, Kantarci K, *et al*. (2013): Elevated occipital beta-amyloid deposition is associated with widespread cognitive impairment in logopenic progressive aphasia. J Neurol Neurosurg Psychiatry 84:1357–1364.
12. Sepulcre J, Sabuncu MR, Becker A, Sperling R, Johnson KA (2013): In vivo characterization of the early states of the amyloid-beta network. Brain 136:2239–2252.
13. Bullmore E, Sporns O (2009): Complex brain networks: Graph theoretical analysis of structural and functional systems. Nat Rev Neurosci 10:186–198.
14. Jack CR Jr, Lowe VJ, Weigand SD, Wiste HJ, Senjem ML, Knopman DS, *et al*. (2009): Serial PIB and MRI in normal, mild cognitive impairment and Alzheimer's disease: Implications for sequence of pathological events in Alzheimer's disease. Brain 132:1355–1365.
15. Villemagne VL, Burnham S, Bourgeat P, Brown B, Ellis KA, Salvado O, *et al*. (2013): Amyloid β deposition, neurodegeneration, and cognitive decline in sporadic Alzheimer's disease. a prospective cohort study. Lancet Neurol 12:357–367.
16. Ossenkoppele R, van der Flier WM, Zwan MD, Adriaanse SF, Boellaard R, Windhorst AD, *et al*. (2013): Differential effect of APOE genotype on amyloid load and glucose metabolism in AD dementia. Neurology 80:359–365.
17. Chare L, Hodges JR, Leyton CE, McGinley C, Tan RH, Kril JJ, Halliday GM, *et al*. (2014): New criteria for frontotemporal dementia syndromes: clinical and pathological diagnostic implications. J Neurol Neurosurg Psychiatry 85:865–870.
18. Rowe CC, Ellis KA, Rimajova M, Bourgeat P, Pike KE, Jones G, *et al*. (2010): Amyloid imaging results from the Australian Imaging, Biomarkers and Lifestyle (AIBL) study of aging. Neurobiol Aging 31:1275–1283.
19. Mioshi E, Dawson K, Mitchell J, Arnold R, Hodges JR (2006): The Addenbrooke's Cognitive Examination Revised (ACE-R): A brief cognitive test battery for dementia screening. Int J Geriatr Psychiatry 21:1078–1085.
20. Savage S, Hsieh S, Leslie F, Foxe D, Piguet O, Hodges JR (2013): Distinguishing subtypes in primary progressive aphasia: Application of the Sydney language battery. Dement Geriatr Cogn Disord 35:208–218.
21. Bullmore ET, Bassett DS (2011): Brain graphs: Graphical models of the human brain connectome. Annu Rev Clin Psychol 7:113–140.
22. Peng J, Wang P, Zhou N, Zhu J (2009): Partial correlation estimation by joint sparse regression models. J Am Stat Assoc 104:735–746.
23. Whittaker J (1990): Graphical Models in Applied Multivariate Statistics. New York: Wiley, pp 241–260.
24. Newman ME (2003): The structure and function of complex networks. SIAM Rev 45:167–256.
25. Rubinov M, Sporns O (2010): Complex network measures of brain connectivity: Uses and interpretations. Neuroimage 52:1059–1069.
26. Newman ME (2002): Assortative mixing in networks. Phys Rev Lett 89: 208701.
27. Watts DJ, Strogatz SH (1998): Collective dynamics of 'small-world' networks. Nature 393:440–442.
28. Linton CF (1977): A set of measures of centrality based on betweenness. Sociometry 40:35–41.
29. Madhavan A, Whitwell JL, Weigand SD, Duffy JR, Strand EA, Machulda MM, *et al*. (2013): FDG PET and MRI in logopenic primary progressive aphasia versus dementia of the Alzheimer's type. PLoS One 8:e62471.
30. Oh H, Mormino EC, Madison C, Hayenga A, Smiljic A, Jagust WJ (2011): β-Amyloid affects frontal and posterior brain networks in normal aging. Neuroimage 54:1887–1895.
31. La Joie R, Perrotin A, Barre L, Hommet C, Mezenge F, Ibazizene M, *et al*. (2012): Region-specific hierarchy between atrophy, hypometabolism, and beta-amyloid (Abeta) load in Alzheimer's disease dementia. J Neurosci 32:16265–16273.
32. Chetelat G, Villemagne VL, Bourgeat P, Pike KE, Jones G, Ames D, *et al*. (2010): Relationship between atrophy and beta-amyloid deposition in Alzheimer disease. Ann Neurol 67:317–324.
33. Becker JA, Hedden T, Carmasin J, Maye J, Rentz DM, Putcha D, *et al*. (2011): Amyloid-beta associated cortical thinning in clinically normal elderly. Ann Neurol 69:1032–1042.
34. Scheinin NM, Aalto S, Koikkalainen J, Lotjonen J, Karrasch M, Kemppainen N, *et al*. (2009): Follow-up of [11C]PIB uptake and brain volume in patients with Alzheimer disease and controls. Neurology 73: 1186–1192.
35. Thal DR, Capetillo-Zarate E, Del Tredici K, Braak H (2006): The development of amyloid beta protein deposits in the aged brain. Sci Aging Knowledge Environ 2006:re1
36. Rijal Upadhaya A, Kosterin I, Kumar S, von Arnim CAF, Yamaguchi H, Fändrich M, *et al*. (2014): Biochemical stages of amyloid-β peptide aggregation and accumulation in the human brain and their association with symptomatic and pathologically preclinical Alzheimer's disease. Brain 137:887–903.
37. Lu JX, Qiang W, Yau WM, Schwieters CD, Meredith SC, Tycko R (2013): Molecular structure of beta-amyloid fibrils in Alzheimer's disease brain tissue. Cell 154:1257–1268.

38. Murray ME, Lowe VJ, Graff-Radford NR, Liesinger AM, Cannon A, Przybelski SA, *et al*. (2015): Clinicopathologic and 11C-Pittsburgh compound B implications of Thal amyloid phase across the Alzheimer's disease spectrum. Brain 138:1370–1381.
39. Rogalski EJ, Rademaker A, Harrison TM, Helenowski I, Johnson N, Bigio E, *et al*. (2011): ApoE E4 is a susceptibility factor in amnestic but not aphasic dementias. Alzheimer Dis Assoc Disord 25:159–163.
40. Wolk DA, Dickerson BC (2010): Apolipoprotein E (APOE) genotype has dissociable effects on memory and attentional-executive network function in Alzheimer's disease. Proc Natl Acad Sci U S A 107: 10256–10261.
41. Josephs KA, Duffy JR, Strand EA, Machulda MM, Senjem ML, Lowe VJ, *et al*. (2014): APOE epsilon4 influences beta-amyloid deposition in primary progressive aphasia and speech apraxia. Alzheimers Dement 10:630–636.
42. Leyton CE, Hodges JR, McLean CA, Kril JJ, Piguet O, Ballard KJ (2015): Is the logopenic-variant of primary progressive aphasia a unitary disorder? Cortex 67:122–133.
43. Drzezga A, Grimmer T, Henriksen G, Muhlau M, Perneczky R, Miederer I, *et al*. (2009): Effect of APOE genotype on amyloid plaque load and gray matter volume in Alzheimer disease. Neurology 72: 1487–1494.